Introduction

Hydraulic fracturing (HF) techniques induce in low-porosity unconventional reservoirs artificial fracture networks for optimizing the production. A number of efficient monitoring techniques, such as downhole or surface passive microseismic methods have been developed to study the deformation processes in a hydraulically stimulated reservoir. In practice, downhole microseismic monitoring is often undertaken using an array of geophones installed in a single monitor well (e.g. [2]). This acquisition geometry, although it is subject to a number of limitations that stem from limited observational aperture, relies on the advantage of the receiver locations in close proximity to the treatment zone ([5]). Hypocentres of microseismic events are typically computed by picking the P- and S-wave arrival times, computing the least-squares fit to the picked times based on a site-specific velocity model, and estimating the azimuth from the receiver to the event by polarization analysis of the P wave (e.g. [6]). Although some automation of this process can be achieved, it nevertheless requires a significant level of user interaction, and is prone to missing events for which only a single-phase (e.g. the S-wave) is readily discernible.
Template-based methods (also known as Matched Filtering Analysis, or MFA) have been developed for automated detection of weak events in earthquake studies (e.g. [7]) and recently employed for microseismic monitoring (e.g. [4]). In this paper we describe a recently developed MFA method [3] which is mainly based on cross-correlation of the raw continuous time series with a template event, herein referred to as a 'parent', yielding times, locations and magnitudes of additional 'child' events.

Our MFA method

The core of the MFA method is cross-correlation between parent events and raw data, which generates automatically child events on the basis of waveform similarity. We have developed optimal strategies defining parent events or from an existing contractor catalog or by standard algorithm detection. Our approach requires a set of accurately located parent events with good signal-to-noise ratio (SNR). Preconditioning is required for both parent events and raw data to avoid spurious detections and to ensure sufficient sensitivity for detection of low SNR child events. Signal preconditioning consists in normalizing parent events by their maximum three-component (3C) amplitude, and applying an automatic gain control (AGC) function to the raw data using a window length similar to the event duration. After the cross-correlation which is performed component by component, child detections are obtained by selection of local maxima of the stacked cross-correlation function over all the receivers. The detection threshold is based on exceedence of a user-specified multiple of the standard deviation of the stacked function. Using this approach, different parent events can be correlated with the same child event; therefore it is mandatory to remove duplicate child events. This action is performed by retaining the parent-child pair associated with the highest peak cross-correlation amplitude. The location of a child event relative to its parent is determined using an automated process, by rotation of the multi-component waveforms into the ray-centered co-ordinates of the parent P, S_{fast}, S_{slow} components. Following, the energy of the stacked amplitude envelope of a reference phase child trace (P or S_{fast}) is maximized within a search volume around the parent's hypocentre, using a search-grid procedure which excluded events located outside the grid. Child locations are anchored by locations of the corresponding parent event; this approach enables determination of hypocentres of single phase events (i.e. only S- or P-wave is detected). After correction for geometrical spreading and attenuation, the relative magnitude of the child event is obtained automatically using the ratio of the stacked envelope peak with respect to its parent.

Results of the MFA method

The sensitivity detection of the MFA method has been tested on a set of microseismic synthetic signals and applied on a real microseismic experiment ([1]) conducted in the Garrington pool (Cardium) in western Canada.

Figure 1 shows the study area where the major hydrocarbon pools are indicated. Figure 2 shows three component record sections for a parent event of known magnitude -1.94 ((a) and (b)) and obtained magnitudes of a child events with the MFA method, -2.46 ((c) and (d)). In (a) and (c) traces are plotted

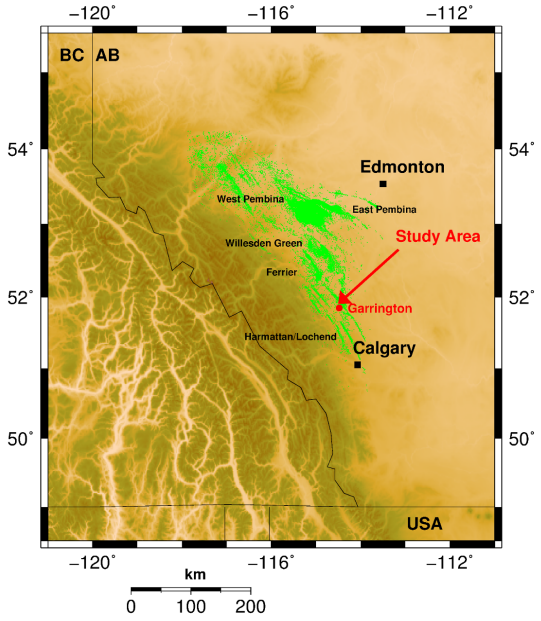

Figure 1 *Location map of the microseismic experiment in western Canada and major hydrocarbon pools*

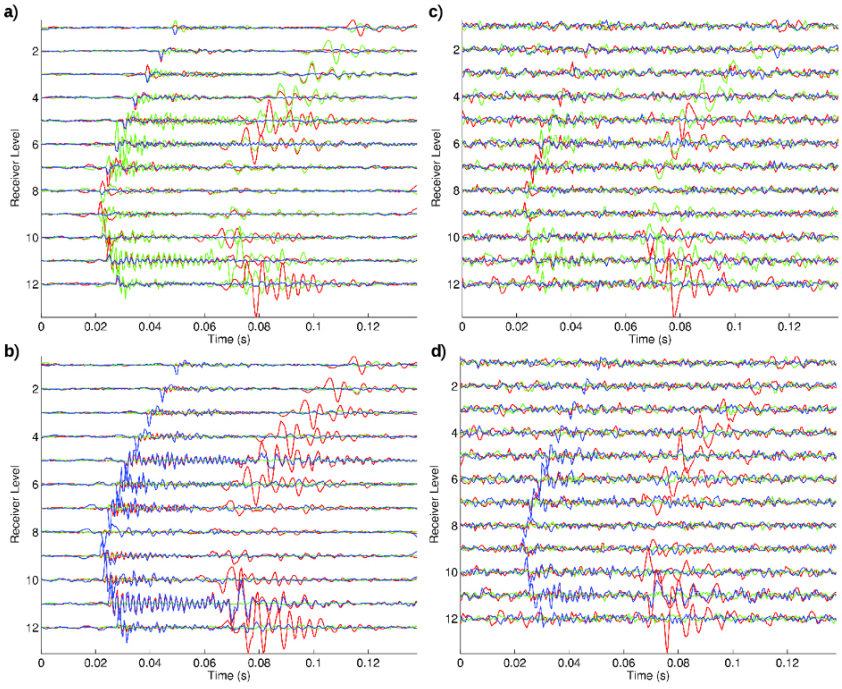

Figure 2 *Parent ((a), (b)) and child ((c), (d)) traces obtained with the MFA method. (a) and (c) traces are not rotated, (b) and (d) traces are rotated in the polarization vectors of the ray-centered coordinate of the parent.*

using the original receiver (geophone) orientations without any rotation (h1 = red, h2 = green, z = blue). In (b) and (d), traces are projected onto the polarization vectors of the parent event (P = blue, S1 = red, S2 = green). This projections results in approximate separation of P, S_{fast} and S_{slow} wavefields (from

[3]). Commercial processing of the Garrington dataset yielded a complex spatial distribution of microseismicity ([1]), with 346 microseismic events in HF stages 1-4 in a magnitude range from -4.01 to

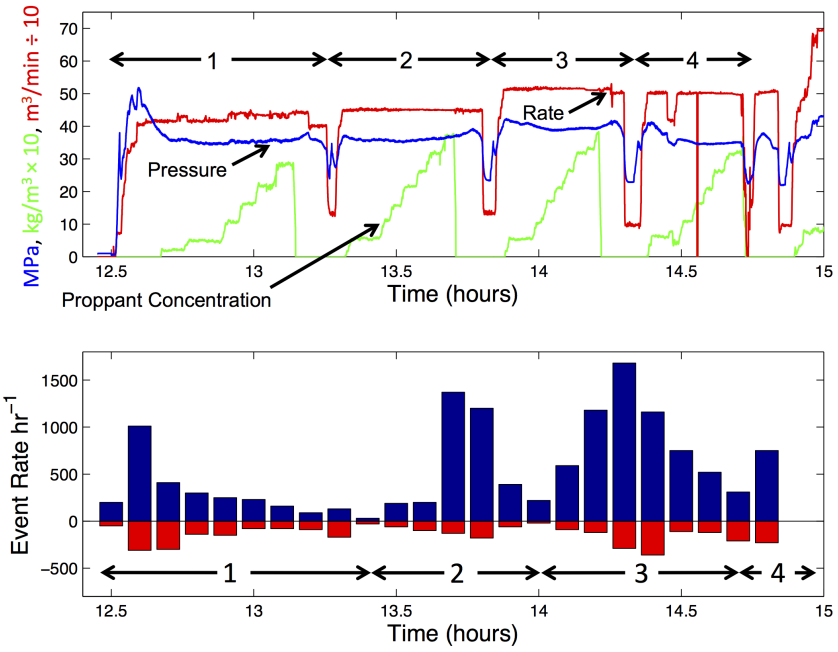

Figure 3 *Comparison between treatment curves (upper panel) with microseismicity rate (lower panel) for both the original catalog (red) and the MFA method (blue).*

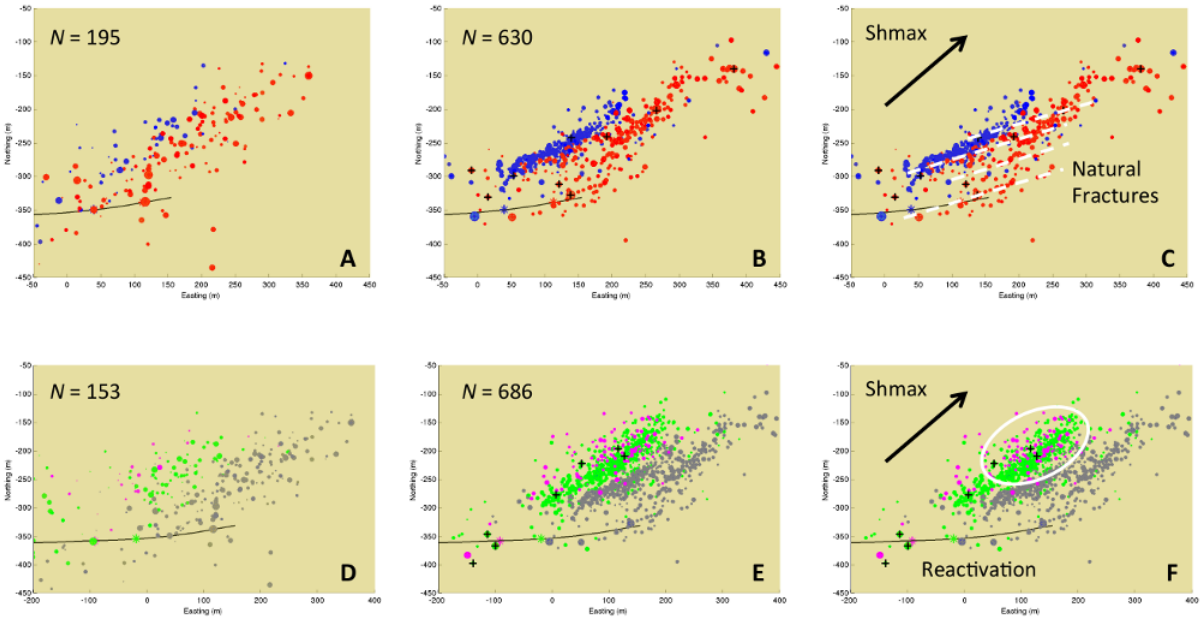

Figure 4 *Map view of the microseismicity clusters from Figure 3: A. original catalogue for clusters 1 (red) and 2 (blue); B. MFA catalogue results (clusters 1 and 2); D original catalogue for clusters 3 (green) and 4 (magenta); E MFA results (clusters 3 and 4). C. and F. are attempts of interpreting B. and E. respectively*

.

-1.29.
Four events from each treatment stage were chosen here as parent events, based on criteria of high SNR and avoidance of pairs of parent events in the same parent-child family. Parent locations and magnitudes are based on the original contractor processing of the data. After removal of duplicate child events, we detected and located 1316 child events. In Figure 3, the microseismic event rate is shown (bottom) and compared with the treatment curves (top). The event rate for the MFA results is plotted using blue bars,

and the event rate from the original catalog using red bars. Although both catalogs exhibit approximately similar relative trends in microseismicity, the MFA results are more easily interpreted due to the higher event rate and greater range of values.
We decided to construct clusters of microseismicity based on their rise and fall time obtained with the MFA method instead of following the classical approach of considering the HF stage time. Figure 4 shows a map view of the microseismicity obtained in this manner from A the original and B MFA catalogues for clusters 1 (red) and 2 (blue). The equivalent for clusters 3 (green) and 4 (magenta) is shown in D and E respectively; grey color indicates the two previous clusters. For all the clusters the event symbol size is scaled by magnitude. Although the overall trend of the microseismicity appears to be close to the direction of the regional maximum stress component S_{hmax}, several event lineations extending between clusters suggest activation of natural fractures with an ENE strike, oblique to Shmax (Figure 4 C.). Cluster 4 contains a part of events that reactivated (Figure 4 F.) from a distal part of cluster 3 during a pressure transient that occurred after stage 4 (see Figure 3). It appears evident that our MFA method is capable to provide insights on HF completion efficiency and activation of existing natural fractures, therefore contributing in understanding deformation processes in stimulated reservoirs.

Conclusions

We have developed a Matched Filtering Algorithm (MFA) currently designed for application to downhole microseismic monitoring using an array of multi-component receivers within a single monitor well [3]. Our method is based on cross-correlation between reference events ('parent') and continuous raw data, generating additional ('child') events. A new technique based on projection of child events on to ray-centered coordinates of the corresponding parent permits a reliable estimation of the child relative magnitudes and locations, including single-phase events. Hypocentre locations of child events are obtained by maximizing the amplitude of stacked envelope functions within a user-defined volume centered in the parent hypocentre. Application of our MFA procedure to four stages from a hydraulic-fracturing treatment in western Canada resulted in a roughly 4-fold increase in the number of located events relative to recently processed ($\sim$ 2 years) data. We compared the microseismicity with the hydraulic-fracture treatment curves and identified temporal clusters. MFA results appear to provide a more reliable basis for interpretation of the spatio-temporal evolution of the microseismicity and insight on HF completion efficiency.

Acknowledgements

This work was funded by the Microseismic Industry Consortium and a Collaborative Research and Development grant from the Natural Sciences and Engineering Research Council of Canada.

References

[1] Duhault, J., 2012. Cardium microseismic west central Alberta: a case history. *CSEG Recorder*, October, 48-57.
[2] Eaton, D.W., Caffagni, E., Rafiq, A., van der Baan, M., and Roche, V., 2014a. Passive seismic monitoring and integrated geomechanical analysis of a tight-sand reservoir during hydraulic-fracture treatment, flowback and production. *URTeC*, 1929223.
[3] Eaton, D.W. and Caffagni, E., 2015. Enhanced downhole microseismic processing using matched filtering analysis (MFA). *First Break*, **33**, 33-39.
[4] Goertz-Allmann, B.P., Kuehn, D., Oye, V., Bohloli, B., and Aker, A., 2014. Combining microseismic and geomechanical observations to interpret storage integrity at the In Salah CCS site. *Geoph. J. Int.*, **198**, 447-461.
[5] Maxwell, S.C., Rutledge, J., Jones, R., and Fehler, M., 2010. Petroleum reservoir characterization using downhole microseismic monitoring, *Geophysics*, **75**, 75A129-75A137.
[6] Oye, V. and Roth, M., 2003. Automated seismic event location for hydrocarbon reservoirs, *Comp. and Geosc.*, **29**, 851-863.
[7] Skoumal, R.J., Brudzinski, M.R., and Currie, B.S., 2015. Earthquakes induced by hydraulic fracturing in Poland Township, Ohio. *Bull. Seism. Soc. Am.*, **105**, 1-8.